UDC 538.9, 53.044, 53.043, 544.72

RESISTANCE OF FINE SINGLE-WALL CARBON NANOTUBES, HIGHLY ORIENTED PYROLYTIC GRAPHITE, AND REDUCED GRAPHENE OXIDE IN COMPOSITES WITH POLYSTYRENE

Nikolaeva M.N.[1], Dunaevskiy M.S.[2], Gushchina E.V.[2], Bugrov A.N.[1, 3]
[1]NRC "Kurchatov Institute" - PNPI-IMC St. Petersburg, Russia,
[2] Ioffe Institute, St. Petersburg, Russia
[3]Department of Physical Chemistry, Saint-Petersburg Electrotechnical University, St. Petersburg, Russia

🖂Marianna_n@mail.ru, anbugrov@etu.ru, mike.dunaeffsky@mail.ioffe.ru, katgushch@yandex.ru

PACS: 36.20.-r; 68.65.Pq; 71.20.Rv; 72.80. Tm; 74.78.-w

Relatively low resistance values were obtained in certain areas of the surface of single-walled carbon nanotubes and highly oriented pyrolytic graphite in metal/polymer composite/metal systems, and these values were compared with the resistance values of reduced graphene oxide aggregates embedded into the similar polymer matrix. Reduced graphene oxide, single-walled carbon nanotubes, and highly oriented pyrolytic graphite were introduced into composites during styrene radical polymerization and after their surface modification. The resistance decreased for composites in the range: single-walled carbon nanotubes, highly oriented pyrolytic graphite, reduced graphene oxide, reaching extremely low values for the latter when was measured in planar metal/carbon derivative/metal structures. Also, comparing the resistance values in the electrode structures of different geometries, it was determined that for carbon additives under study in planar structures resistance values are lower by several orders of magnitude than the resistance in sandwich structures, and is also lower than the resistance of highly conductive metals. Such a decrease in the resistance values of carbon inclusions can be explained by the formation of a new mutual orientation of carbon particles during syntheses and later by changes under deformation stresses between them and the polymer matrix during composites films' preparation. We proposed that these processes can possibly affect the electronic structure of the carbon derivatives.

Keywords: single-walled carbon nanotubes, highly oriented pyrolytic graphite, reduced graphene oxide, polymer composites, resistance, superconductivity.

For a plenty of industries it is of great importance to use superconducting materials with a high critical temperature (T_c), i.e., demonstrating superconductive state up to room temperatures and even higher. As perspective materials for practical use can be considered carbon derivatives which are very light and rather cheap. It was assumed in [1 - 3] that the effect of such an anomalous decrease of resistance values could be associated with deformation shifts and stresses in some areas of reduced graphene oxide (rGO) surface, when carbon inclusions are introduced into the polymer matrix during syntheses and form covalent bonds with it. A study of the magnetic properties of graphene-containing composites on a vibrational magnetometer showed the existence of superconductivity effect in rGO [3] and superconducting particles can be separated from the others particles of rGO in the polymer composite [4].

At the same time, signs of superconductivity were also registered for finely dispersed highly oriented pyrolytic graphite (HOPG) [5] and other carbon compounds that do not form covalent bonds with the environment [6-11]. It should be noted that the high-temperature superconductivity has been achieved at graphite interfaces [12], and in disordered carbon [13]. Unlike rGO, which forms covalent bonds with polystyrene as a result of copolymerization [2], HOPG and single-walled carbon nanotubes (SWCNTs) in composites with polystyrene should be, first, linked with polymer by van der Waals forces, since they do not have a significant number of functional groups on its surface capable to form the chemical bonds with polystyrene. The previously obtained values of anomalously low resistance, in particular, for multilayer rGO [1-4], as well as the capture of the magnetic moment by finely dispersed HOPG [10], suggest that they are associated with a change in the surface topology and mutual orientation of carbon nanoparticles. Since the effect of deformation interactions leading to the appearance of superconducting properties was previously pointed out in rGO after syntheses with polystyrene [1-4], it seems likely that the process of copolymerization with styrene should also create some deformation stresses on the surface of SWCNTs and HOPG although in a lesser extent. So, conductive properties of finely dispersed HOPG and SWCNTs creating a small amount of covalent bonds with a polymer matrix could be different from conductive properties of rGO having a plenty of covalent bonds with a polymer. Besides additional changes of the number and the strength of bonds between carbon fillers and the polymer matrix apparently should be caused by the grinding and diminishment of carbon additives, namely SWCNTs and HOPG, since the mutual orientation of graphene layers could be shifted under grinding, and new defects can appear at the edges of carbon sheets. It is obviously that with a large decrease of carbon particles' sizes under intense grinding of their host composites the influence of quantum effects can increase as well.

The study of the superconductivity phenomenon of carbon nanostructures in polymer composites, as well as the development of electronic devices based on them with extremely high sensitivity to magnetic flux (SQUIDs), makes not only a significant contribution to the evolution of fundamental ideas about the superconducting state, but also has prospects for practical application in spintronic. In addition, the development of technology of high-temperature superconductors will simplify and reduce the cost of a wide range of medical research. In particular there should be mentioned the possible prospects for the early diagnostics of cancer diseases. It is determined that cancer cells and tumors create electromagnetic fields that is different from electromagnetic fields of healthy surrounding tissues. According to this assumption, facts concerning the interaction of tumor cells with an external electromagnetic field and nerve cells of the body are found [14, 15]. Besides this, the proximity of nerve endings to each other and their increased electromagnetic field strength influencing the nearest somatic cells can be considered as the trigger for the emergence of cancer cells. As it is known, a strong electric field can change the geometry of molecules and polarize their orbitals [16-18]. As a result, a strong polarization of DNA fragments is possible, which can lead to serious failures in the functioning of critically important gens, and, as a result, to the possible creation of cancerous formations. The differences in the magnitudes of electromagnetic fields of cancerous and healthy tissues can be detected in perspective by supersensitive superconducting magnetometers with a high T_c [19-21] especially when the development of methods of electromagnetic noise suppression will be achieved.

Since the theory [22-24] predicts the possibility of the room-temperature superconductivity for deformed carbon sheets the aim of this paper is to find other perspective carbon derivatives for room-temperature superconductivity and for this to measure the resistance values of SWCNTs, HOPG and rGO in their polymer composites after deformation stresses.

EXPERIMENTAL PART

The studied SWCNTs from the manufacturer OCSiAl had an individual nanotube length of more than 5 μm, an outer average diameter of 1.4 ± 0.3 nm, and an outer specific surface area of about 400 m^2/g. At the same time nanotubes form stable bunches of real lengths of some tens and hundreds micrometers as was shown by SEM method (Fig.1, a).

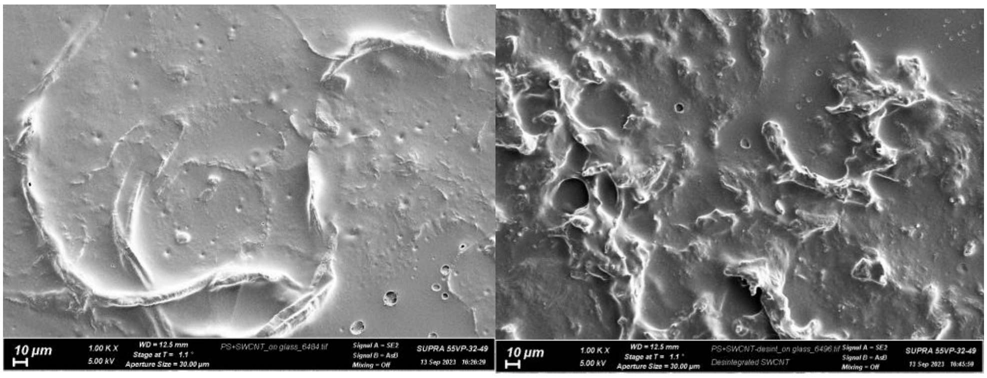

a b

Fig.1. SEM micrographs of the films' surface of polystyrene composite with original (a) and crushed (b) SWCNTs [25]

The type of the used HOPG is ZYA_DS (https://www.ntmdt-tips.com/products/group/zya), the size of the original piece of HOPG is 0.7x0.7x0.3 mm.

The rGO was obtained from native crystalline graphite due to an oxidation followed by a reduction using the modified Hummers method [26].

Next, the every of carbon compounds were treated with a silicon-containing compound 3-(trimethoxysilyl) propyl methacrilate (TMSPMA) from Sigma-Aldrich, >98% purity, and introduced into a polystyrene mixture during radical polymerization with styrene (Sigma-Aldrich, >99% purity) using an azobisisobutyronitrile initiator (Fluka, >98% purity) [27]. A method of composites synthesizing is described in [2]. The content of rGO, SWCNTs, and HOPG in the synthesized composites was 1 wt %. Syntheses of all 3 composites continued for 20 hours, as a result, the polymer yield was more than 90%, and the molecular weight of polystyrene was about 14500 Da. Macroscopic HOPG samples have been mechanically ground before synthesis with styrene with a glass rod in a glass beaker for 1 hour. After precipitation in ethanol and drying, the resulting PS/SWCNT composite was mechanically crushed in a vibrating ball mill (DDR-GM 9458, 30 W, 50 Hz, Germany) for 1 hour to a powdery state and then further crushed with a glass rod in a glass beaker for 2 hours. The grinding was continued until the length of the individual particles of SWCNTs did not exceed 5-10 μm, and some of them did not reach the size of about 1 μm (Fig. 1, b). The composite with rGO was not subjected to grinding, since the sizes of individual rGO particles in the polymer matrix after synthesis were about 5-8 μm, even without grinding. Thus, all carbon additives in the polymer matrix originally had linear dimensions in the range of about 0.5 to 10 μm.

To obtain current-voltage characteristics (CVCs) of the composites in metal/composite/metal sandwich structures, the composites were deposited on copper electrodes from their 1 wt. % benzene solutions. The copper electrode diameter was about 0.5 cm^2. The thicknesses of the films deposited on the electrodes were 2 μm and were estimated using an interference microscope, as in [2]. The current-voltage characteristics (CVCs) and temperature dependencies of the resistance in metal/composite/metal both in sandwich and planar structures were obtained by the modified four probe method, as in [2, 28] with 2-probe and 2-current contacts.

For measuring CVCs in planar structures, the composites were deposited on a glass substrate from a benzene/petroleum ether solvent mixture in a 1:1 ratio by volume. Chemically pure benzene and petroleum ether 40-70 (ECOS-1) were used to prepare composite solutions. It was shown previously [2] that this ratio allows the maximum separation of rGO and polystyrene, and contributes to the maximum enlargement of carbon agglomerates on the polymer surface. To obtain sufficiently large SWCNT structures on the surface of polystyrene deposited from such a mixture of solvents, solutions were prepared with a composite content of about 30 wt %.

The surface topography and local current maps were measured using atomic force microscopy (AFM). Conductive AFM method (c-AFM) allowed to obtain simultaneous of two-dimensional (2D) surface and local current maps of the film. This allows comparing topography and local current signals along a selected line. The upper electrode was an AFM probe with a 20-30 nm thick conductive Pt coating (HA_C/Pt) ("TipsNano"). Probe stiffness is ~0.5 N/m, and the probe curvature radius is R~15-20 nm. The quality of the Pt coating on the probe was checked before each measurement.

Temperature dependencies of resistance were obtained in sandwich structures in the temperature range of 90 – 298 K for composites' films with thickness 2 μm.

RESULTS AND DISCUSSION

During precipitation with petroleum ether from a benzene solution sufficiently large rGO agglomerates were formed on a polystyrene surface (Fig. 2). It would be due to the fact that rGO has a low density, is subjected to exfoliation, and can be easily reoriented when polymer coils are compressed in a poor solvent. For SWCNTs (Fig. 3), this effect of SWCNT inclusions' enlargement is less marked, since a precipitation with petroleum ether practically does not influence sizes of carbon inclusions. The area of SWCNT aggregates in this case enlarges mainly due to an increase of SWCNT concentration up to 30 wt %. The composite with SWCNTs deposited on glass plates consisted of SWCNTs inclusions of different sizes in the polymer matrix, their maximum sizes were reaching 0.5 mm. Such sizes of inclusions made it possible to measure their resistance on the polymer surface. In the case of HOPG (Fig. 4), the use of petroleum ether did not give the effect of a size increase of HOPG inclusions at all, neither deposited from benzene solutions nor deposited from a benzene/petroleum ether mixture. For this reason, since it was not possible to obtain planar structures for HOPG, measurements of the CVCs and temperature dependencies of the resistance were carried out only in sandwich structures. Apparently, HOPG particles in the polymer matrix after synthesis and ultrasonic exposure during synthesis are scattered and are not able to aggregate into large formations when petroleum ether is used as a precipitant for polystyrene. Beside this, HOPG particles are practically immersed in the thickness of the polymer and do not come out to the surface of sufficiently thick polystyrene films (up to 30 μm thick and more). Thus they are inaccessible for CVCs measuring in planar structures because at the high concentration of the composite in a solvent mixture (~30 wt %), polymer films always had a thickness of tens of micrometers.

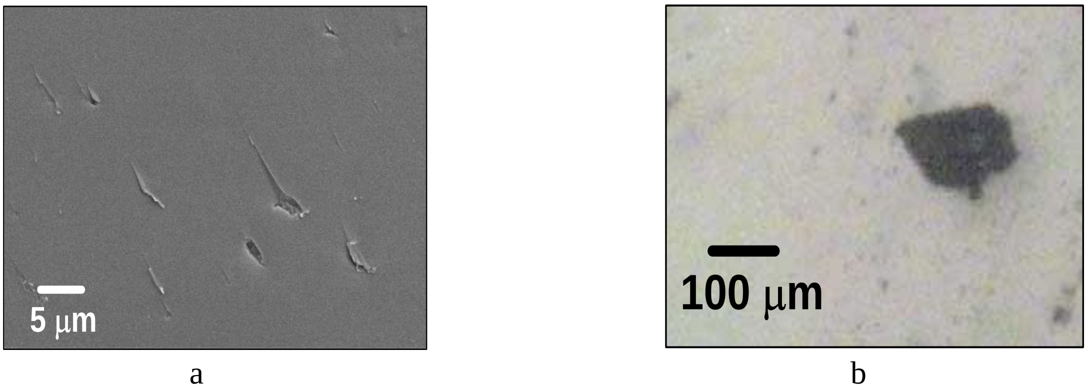

a b

FIG. 2. SEM image (a) of rGO distribution in polystyrene matrix without using precipitation and optical image (b) of some rGO flakes on polystyrene matrix formed after precipitation [2]

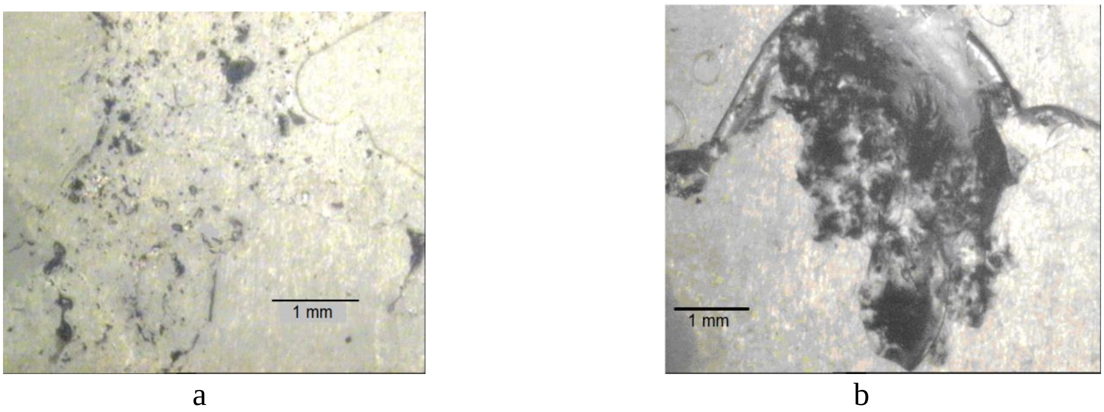

Fig. 3. Microphotos of composite films with ground SWCNTs on a glass substrate deposited from: a – benzene solution, 1 wt.%; b – benzene / petroleum ether mixture, 30 wt.%

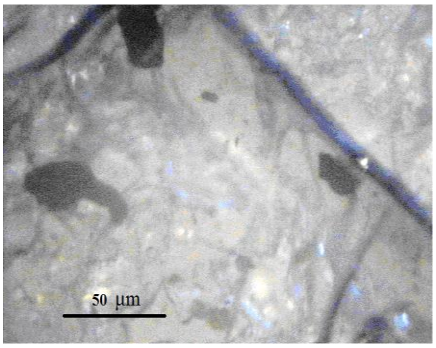

Fig. 4. Optical image of some HOPG flakes in polystyrene matrix

Since most areas of the composite films are highly resistive, the data shown in Figure 6 refer to the carbon-containing areas with the lowest resistance values. Current-voltage characteristics in sandwich structures for polystyrene composites with rGO, HOPG and SWCNTs are shown in Fig. 5. The current-voltage characteristics obtained for rGO and SWCNTs in planar structures are shown in Fig. 6.

The studied carbon compounds demonstrate resistance values that differ by 1-2 orders of magnitude. So, in sandwich structures at room temperatures resistance for rGO was in average about 0.25 Ώ, for HOPG - about 0.6 Ώ and for SWCNTs - about 13 Ώ (Fig. 5). At the same time, copper electrodes without coating in such sandwich structures have resistance values near 0.13 Ώ. Such difference between resistance values of carbon derivatives could be explained by some changes in the chemical structure and a possible different degree of carbon sheets’ deformations in composites under study. Besides the formation of a newly ordered and enlarged carbon structures under the influence of petroleum ether in planar structures can cause additional influence on the process of a self-structuring of small particles of rGO and SWCNTs. It is worth to mention that in composite films with SWCNTs and rGO in planar structures, the dots demonstrating a very low resistance were observed only on areas of large carbon inclusions (up to hundreds of micrometers). Thus, in planar structures at room temperatures resistance for rGO was about 20 kΏ and for SWCNTs - about 430 kΏ (Fig. 6). For comparing of resistance values of carbon derivatives with metals, resistance of pure copper and gold samples of close geometry were measured by the same electrodes at room temperature and resistance values of both metals were about 3 MΏ. Since resistance values is directly dependent on contact area one can see that resistance of gold and copper is higher than resistance of some places of our carbon derivatives in planar structures.

Resistance temperature dependencies show metallic type of conductivity for films of composites with SWCNTs, HOPG and rGO (Fig. 7, 8).

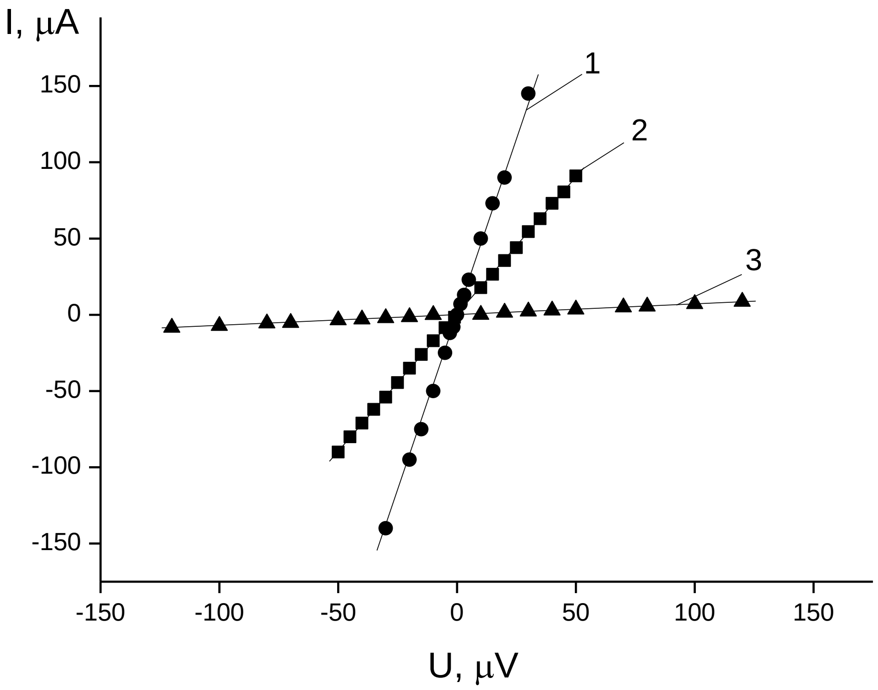

Fig. 5. CVCs of polystyrene composites in sandwich structures with: 1 – rGO, 2 – HOPG, 3 – SWCNTs

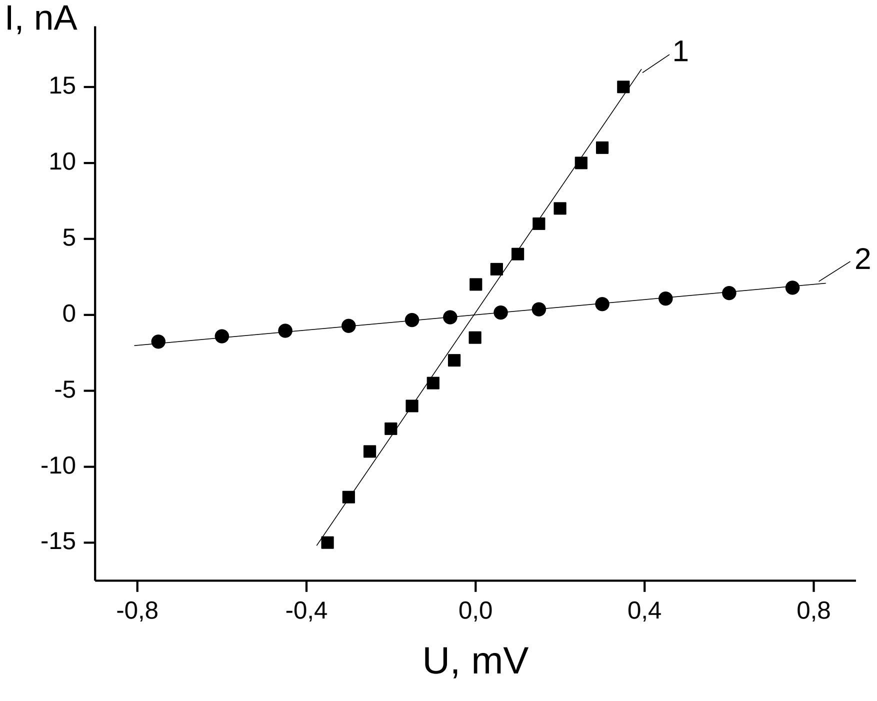

Fig. 6. CVCs of polystyrene composites obtained by AFM probe in planar structures with 1 – rGO and 2 – SWCNTs

It is important to note that when using electrodes even of a large area up to 3 mm^2, the resistance values obtained for a bulk HOPG sample according to literature data [29] were 2 orders of magnitude higher than for our composite films with 1 wt % of HOPG, which have a smaller total surface contact area with the electrodes. It is worth to mention temperature dependencies for bulk and composite HOPG significantly differ from each other. Thus for a composite films with dispersed HOPG the drop in resistance with decreasing temperature from room to nitrogen temperatures was even somewhat faster than for such metals as copper and gold. Thus, in the studied temperature range for the composite with HOPG, the drops in resistance values were as an example, from 0.6 Ω to 0.06 Ω, for gold from 0.0034 to 0.007 Ω, and for copper from 0.135 to 0.025 Ω, correspondingly. At the same time, for a bulk HOPG sample, on the contrary, the resistance dropped 3 times slower in the same temperature range (Fig. 8).

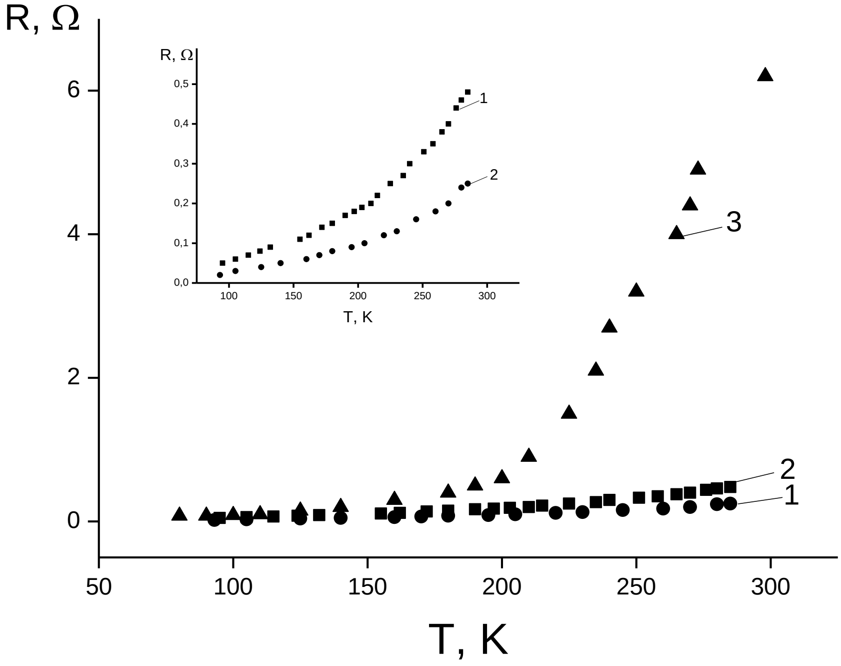

Fig. 7. The temperature dependencies of resistance: 1 – rGO, 2 – HOPG and 3 – SWCNTs, composite film thickness 2 μm

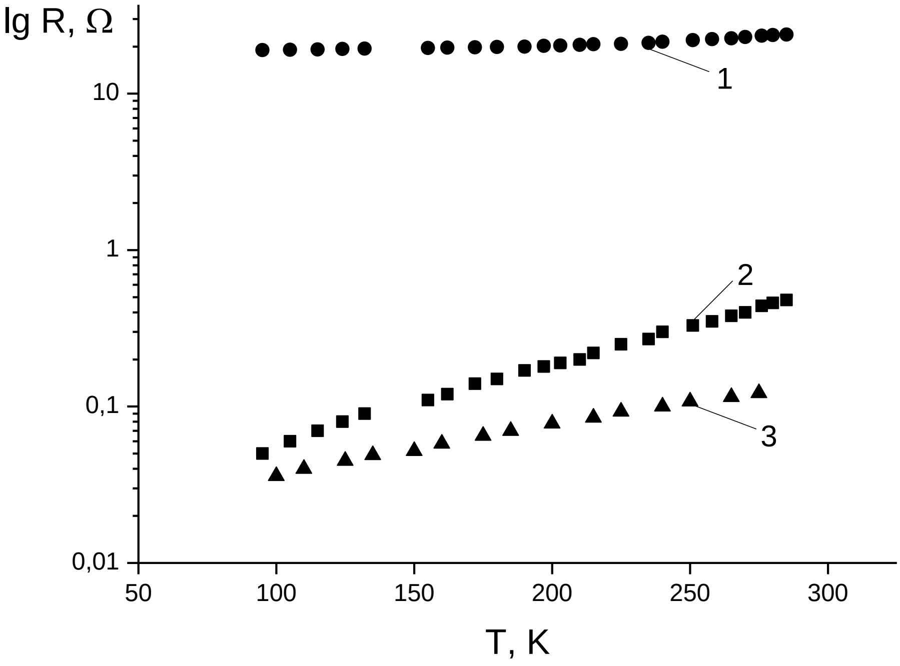

Fig. 8. Decimal logarithm of the temperature dependencies of resistance values for: 1 – the bulk HOPG, 2 - the composite film with HOPG, 3 – copper

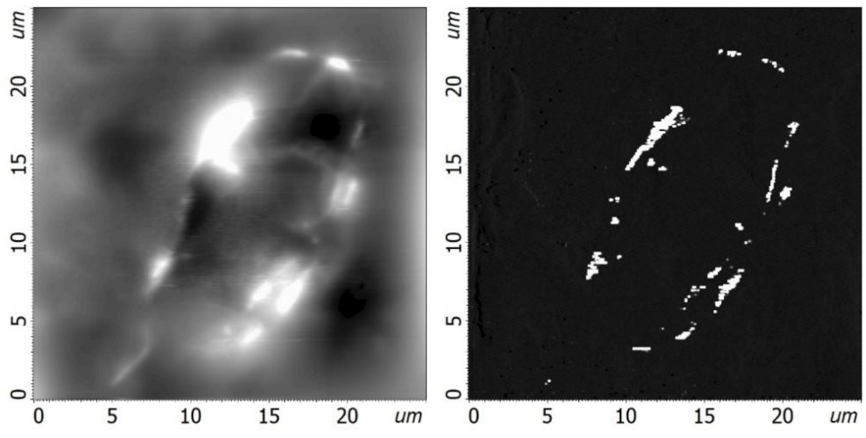

a b

Fig, 9. Polystyrene/rGO composite's: AFM-topography (a) and local current map (b) on gold substrate

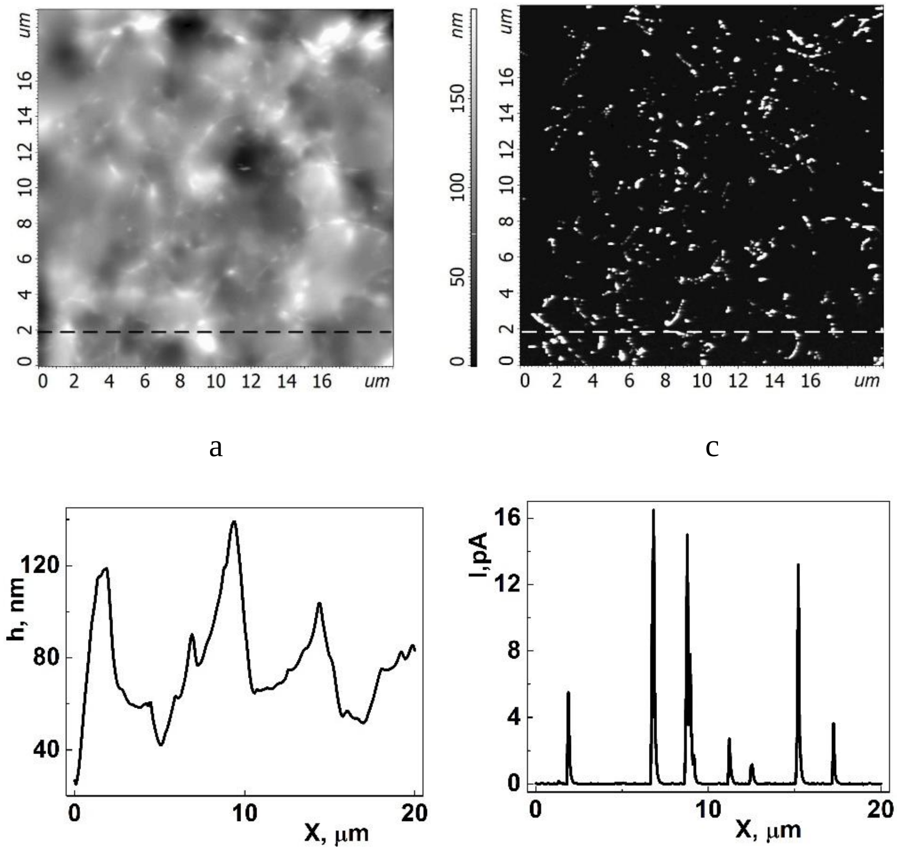

a c

b d

Fig. 10. The modified single walled carbon nanotubes' AFM-topography (a) in polystyrene matrix with surface profile (b) and corresponding local current map (c) with current profile (d)

The influence of deformation changes in carbon sheets on the resistance values of rGO aggregates can be confirmed also by [30] where was shown that conductivity of rGO inclusions in polystyrene matrix correlates with their topography and only some places of rGO highly protruding surface regions were highly conductive (Fig. 9). Deformation of graphene sheets obviously can arise in such bulging areas. It should be noted also that in [4] precisely the different shapes and sizes of rGO particles determined the presence or absence of the superconductivity effect in them. Obviously, the structural features and mutual arrangement of carbon nanoparticles determines the resistance values of the measured carbon structures. This observation is also true for SWCNTs in polystyrene composites (Fig. 10). For bulging areas corresponding current values were several times higher than for plane areas and located in low places.

As was mentioned above, resistance values on R-T dependencies for all three types of composites with SWCNTs, rGO and HOPG sharply decreases according to a temperature decrease. The additional contribution to resistance changes may be due also to the negative expansion coefficient for graphene and graphite, which causes additional deformations of the graphene layers when a temperature decreases, which, in turn, can lead to the influence on resistance values. The presence of surface areas demonstrating anomalously low resistance of the studied carbon structures as well as their resistance temperature dependencies could indicate the possible presence of a special low-resistive component in them, which becomes more and more noticeable at low temperatures. At the same time, for SWCNTs and HOPG, which practically do not have the possibility to form covalent bonds with the polymer matrix, the absolute values of resistance are closer to the corresponding values of metals, i.e. the effect of the appearance of an anomalously low resistance is not as large as in the case of the rGO composite. In the case of a composite with rGO, the resistance in planar structures at room temperatures is 2 orders of magnitude lower than the resistance of gold. The temperature decrease of resistance for rGO was also quicker than for metals, which can also hint the presence of a superconducting component in rGO particles and correlates with results obtained in [3] for analogous rGO composite. So it can be proposed that the more opportunities for a deformation of graphene layers the lower can be resistance values of carbon structures. At the same time in HOPG and SWCNTs, despite lack of functional groups graphene layers can be shifted relative to each other as well during their synthesis with polymer and subsequent grinding. So some local deformation stresses can appear and one can observe anomalously low resistance values in some areas of carbon structures' surface.

CONCLUSIONS

For films deposited from solutions of polymer composites synthesized by the method of radical polymerization of styrene with single-walled carbon nanotubes, highly oriented pyrolytic graphite, and reduced graphene oxide, the current-voltage characteristics and temperature dependencies of the resistance were obtained. The received data demonstrate an anomalously low resistance values in certain areas of the surface when carbon structures were studying in planar structures and the metallic type of conductivity for all carbon additives was determined. At the same time a great difference was found in the resistance values between the rGO composite with covalent bonds and composites with SWCNTs and HOPG, which do not form chemical bonds with polystyrene. In the case of a composite with rGO the resistance values at a room temperatures turned out to be lower by 1-2 orders than for composites with HOPG and SWCNTs both in sandwich structures and in planar structures and the composite with rGO can demonstrate the resistance values even 2 orders of magnitude lower than resistance of metals [2]. For dispersed SWCNTs and HOPG, apparently, this effect of the resistance values' decrease after grinding was obviously marked mostly due to non-covalent interactions, such as van der Waals forces. In these cases a resistance decrease is not as large as in rGO because deformations of carbon sheets can't be as large as for rGO composite. So the changes of the electron density in the local regions of carbon inclusions should be weaker than in rGO which is able to form covalent bonds with polystyrene [1-3].

Thus, for the manifestation of a highly conductive state in carbon particles, it is important to keep special conditions. In particular, these are a presence of chemical functional groups on the surface of carbon derivatives as in rGO and the introduction of carbon additives during the process of synthesis with a polymer leading to deformations of carbon sheets.

The work was carried out on the topic "Polymer and composite materials for advanced technologies", project registration number 124013000726-6.

The authors declare that there is no conflict of interest requiring disclosure in this article.

REFERENCES

1. Ionov A.N. Josephson-Like Behaviour of the Current-Voltage Characteristics of Multi-graphene Flakes Embedded in Polystyrene. J. Low Temp. Phys. 2016, 185 (5-6), P. 515-521. DOI: 10.1007/s10909-015-1459-7
2. Nikolaeva M.N., Bugrov A.N., Anan'eva T.D. Gushchina E.V., Dunaevskii M.S., Dideikin A.T. Resistance of reduced graphene oxide on polystyrene surface. Nanosystems: physics, chemistry, mathematics, 2018, 9 (4), 496–499. DOI: https://doi.org/10.17586/2220-8054-2018-9-4-496-499
3. Ionov A.N., Volkov M.P., Nikolaeva M.N., Smyslov R.Y. Bugrov A.N. The Magnetization of a Composite Based on Reduced Graphene Oxide and Polystyrene. Nanomaterials. 2021, 11 (2), P.403, DOI: https://doi.org/10.3390/nano11020403
4. Ionov A.N., Volkov M.P. Magnetization of Needle Graphene Embedded in a Polystyrene Matrix Tech. Phys. Lett., 2022, 48 (8), P. 44-46, DOI: https://doi.org/10.21883/TPL.2022.08.55060.19179
5. Esquinazi P., Garcia N., Barzola-Quiquia J., Rodiger P., Schindler K.,. Yao J.L, Ziese M. Indications for intrinsic superconductivity in highly oriented pyrolytic graphite. Phys. Rev. B, 2008, (78), P. 134516 (1-8), DOI: https://doi.org/10.1103/PhysRevB.78.134516
6. Buntar V., Weber H. Superconducting properties of fullerenes in the mixed state (A Review). Low Temperature Physics. 1996, 22 (3), P. 177-189, DOI: https://doi.org/10.1063/1.593116
7. Uchoa B., Castro Neto A.H. Superconducting states of pure and doped graphene. Phys Rev Letters, 2007, 98, P. 146801-1 – 146801-4, DOI: 10.1103/PhysRevLett.98.146801
8. Lebedev S.G. Josephson-like behavior of thin granular carbon films. International Review of Physics, 2008, 2 (5), P. 312-328, DOI: https://doi.org/Arxivpreprint con-mat/0706.3310
9. Kopelevich Y, Esquinazi P. Ferromagnetism and superconductivity in carbon-based systems. Low Temp Phys., 2007, 146, P. 629–639, DOI: https://doi.org/10.48550/arXiv.cond-mat/0609497
10. Saad M., Gilmutdinov I.F., Kiiamov A.G., Tayurskii D.A., Nikitin S.I., Yusupov R.V. Observation of Persistent Currents in Finely Dispersed Pyrolytic Graphite. JETP Letters, 2018, 107 (1), P. 37-41, DOI: https://doi.org/10.7868/S0370274X18010083
11. Barzola-Quiquia J., Ballestar A., Dusari S., Esquinazi P. Experimental study of the intrinsic and extrinsic transport properties of graphite and multigraphene samples. Graphene Intech, Open Access Publisher, (Ed: J. R.Gong), 2011, Chap. 8, P.118, DOI: https://doi.org/10.5772/21061
12. Ballestar A. Barzola-Quiquia J., Scheike T., Esquinazi P. Josephson-coupled superconducting regions embedded at the interfaces of highly oriented pyrolytic graphite. New Journal of Physics. 2013, 15 (023024), DOI: https://doi.org/10.1088/1367-2630/15/2/023024
13. Scheike T., Böhlmann W., Esquinazi P., Barzola-Quiquia J., Ballestar A., Setzer A. Can doping graphite trigger room temperature superconductivity? Evidence for granular high-temperature superconductivity in water-treated graphite powder. Adv. Mater., 2012, (24), P. 5826–5831, DOI: https://doi.org/10.48550/arXiv.1209.1938
14. Venkataramani V., Tanev D.I., Strahle C., Studier-Fischer A., Fankhauser L., Kessler T., Körber C, Kardorff M., Ratliff M., Xie R., Horstmann H., Messer M., Paik S.P., Knabbe J., Sahm F., Kurz F.T., Acikgöz A.A., Herrmannsdörfer F., Agarwal A.,. Bergles D., Chalmers A., Miletic H., Turcan S., Mawrin C., Hänggi D., Liu H.-K., Wick W., Winkler F., Kuner T. Glutamatergic synaptic input to glioma cells drives brain tumour progression // Nature. 2019. V. 573. P. 532–538. DOI: https://doi.org/10.1038/s41586-019-1564-x
15. Quicke P., Sun Y., Garcia M.A., Beykou M., Acker C.D., Djamgoz M.B.A., Bakal C., Foust A.J. Voltage imaging reveals the dynamic electrical signatures of human breast cancer cells. Commun Biol. 2022, 11, 5(1), 1178, DOI: 10.1038/s42003-022-04077-2
16. Basch H., Ratner M.A. Molecular binding at gold transport interfaces III. Field dependence of electronic properties. J. Chem Phys., 2004, 120 (12), 5761–5770. DOI: https://doi.org/10.1063/1.1650293
17. Xue Y., Ratner M.A. End group effect on electrical transport through individual molecules: A microscopic study. Phys. Rev. B., 2003, 69 (8), 235410. DOI: https://doi.org/10.1103/PhysRevB.69.085403

18. Mahapatro A.K., Agrawal R., Ghosh S. Electric-field- induced conductance transition in 8-hydroxyquinoline aluminum (Alq_3). J. Appl. Phys., 2004, 96 (6), 3583–3585. DOI: https://doi.org/10.1063/1.1778211
19. Cordani C., Preziosa P., Gatti R., Castellani C., Filippi M., Rocca M.A. Mapping brain structure and function in professional fencers: A model to study training effects on central nervous system plasticity. Human brain mapping, 2022, 1-11. DOI: https://doi.org/10.1002/hbm.25854
20. Gurtovoi V.L., Antonov V.N., Nikulov A.V., Shaikhaidarov R.S., Tulin V.A. Development of a superconducting differential double contour interferometer. Nano Lett., 2017, 17 (11), 6516–6519. DOI: https://doi.org/10.1021/acs.nanolett.7b01602
21. Maslennikov Yu.V. Practice and perspectives of using ultrasensitive magnetometers in biomedical research. Journal of Radio Electronics, 2021, (5), 1684–1719. DOI: https://doi.org/10.30898/1684-1719.2021.5.4
22. Volovik G.E. Graphite, graphene and the flat band superconductivity. JETP Letters, 2018, 107 (8). 516–517. DOI: https://doi.org/10.7868/S0370274X18080131
23. Kopnin N.B., Heikkila T.T. Volovik G.E. High-temperature surface superconductivity in topological flat-band systems. Phys. Rev. B., 2011, 83, 220503 (1-4). DOI: https://doi.org/10.1103/PhysRevB.83.220503
24. Volovik G.E. Flat Band in Topological Matter. J Supercond Nov Magn., 2013, 26, 2887–2890. DOI: https://doi.org/10.1007/s10948-013-2221-5
25. Nikolaeva M.N., Ivan’kova E.M., Bugrov A.N. Nanosystems: Phys. Chem. Math., 2025, 16 (2), 243–249. Conducting properties of single-wall carbon nanotubes in composites based on polystyrene DOI 10.17586/2220-8054-2025-16-2-243-249
26. Aleksenskii A.E., Brunkov P.N., Dideikin A.T., Kirilenko D.A., Kudashova Y.V., Sakseev D.A., Sevryuk V.A., Shestakov M.S., Single-layer graphene oxide films on a silicon surface, Tech. Phys. 58 (11) (2013) 1614–1618
27. Bugrov A.N., Vlasova E.N., Mokeev M.V, Popova E.N., Ivan’kova E.M, Al’myasheva O.V., Svetlichnyi V.M. Distribution of zirconia nanoparticles in the matrix of poly(4,4′-oxydiphenylenepyromellitimide) // Polymer Science, Ser. B, 2012, Vol. 54, Nos. 9–10, P. 486. DOI: http://dx.doi.org/10.1134/S1560090412100041
28. Ionov A.N., Nikolaeva M.N., Rentzsch R. Supercurrent through a polyamidine film // Physica C. 2007. V.460. N 1. P. 641-643. DOI: http://dx.doi.org/10.1016/j.physc.2007.04.141
29. Kawamura K., Ouchi Y., Oshima H. Electrical conduction in c-direction of highly crystalline graphites in relation to structural perfection // J. of the Phys. Soc. of Japan. 1979. V. 46. N. 2. P. 587-593; https://doi.org/10.1143/JPSJ46.587
30. Nikolaeva M.N., Gushchina E.V., Dunaevskii M.S., Dideikin A.T., Bugrov A.N., Anan’eva T.D. The influence of substrate material on the resistance of composite films based on reduced graphene oxide and polystyrene. Nanosystems: physics, chemistry, mathematics, 2017, 8 (5), P. 665–669, DOI 10.17586/2220-8054-2017-8-5-665-669